

Gravity-Sensitive Quantum Dynamics in Cold Atoms

Z.Y. Ma,¹ M.B. d’Arcy,² and S.A. Gardiner³

¹Clarendon Laboratory, Department of Physics, University of Oxford, Oxford OX1 3PU, United Kingdom

²Atomic Physics Division, National Institute of Standards and Technology, Gaithersburg, Maryland 20899-8424, USA

³JILA, University of Colorado and National Institute of Standards and Technology, Boulder, Colorado 80309-0440, USA

(Dated: February 28, 2008)

We subject a falling cloud of cold cesium atoms to periodic kicks from a sinusoidal potential created by a vertical standing wave of off-resonant laser light. By controllably accelerating the potential, we show quantum accelerator mode dynamics to be highly sensitive to the effective gravitational acceleration when this is close to specific, resonant values. This quantum sensitivity to a control parameter is reminiscent of that associated with classical chaos, and promises techniques for precision measurement.

PACS numbers: 05.45.Mt, 03.65.Sq, 32.80.Lg, 42.50.Vk

The identification and observation of signatures of chaos in quantum dynamics is the goal of considerable current effort. Much of this work centers on the theoretical definition and characterization of energy spectra [1], or such quantities as the Loschmidt echo [2] and fidelity [3], which essentially develop the idea that sensitivity of a wavefunction’s evolution to small variations in a system’s Hamiltonian be used as a definition of quantum instability [1, 2, 3, 4]. Such quantities could be observed experimentally but require some interpretation to highlight the way in which their nature betokens stability or chaos. An attractive alternative would be the observation of different motional regimes. This is more in sympathy with the techniques and philosophy used to identify classical chaos, and is the approach used here.

In certain systems the decay of the overlap of two initially identical wavefunctions evolving under slightly differing Hamiltonians can be expressed in the long time limit as the sum of two decay predictions, governed by Fermi’s Golden Rule and the classical Lyapunov exponent [2]. The decay rate serves as a quantum signature of instability, which can be compared with that of the corresponding classical system. Such sensitivity can be probed by interferometric techniques [5, 6]. In the quantum-mechanical system presented here, the classical limit of which is chaotic, extreme sensitivity of the qualitative nature of the motional dynamics to a control parameter is directly observable. It is manifested by the effect on quantum accelerator mode (QAM) dynamics [6, 7, 8, 9, 10] of small variations in the effective value of gravity in the δ -kicked accelerator [7], an extension of the paradigmatic δ -kicked rotor [11]. The QAM observed in this atom optical realization [6, 7, 8, 9, 10], are characterized by a momentum transfer, linear with kick number, to a substantial fraction (up to $\sim 20\%$) of the initial cloud of atoms. This is due to a resonant rephasing effect, dependent on the time-interval between kicks, for certain initial wavefunctions [9, 12]. The sensitivity in the dynamics we observe also promises the capability of precisely calibrating a relationship between the local gravitational acceleration and h/m , where m is the atomic mass, and we describe how our observations constitute a preliminary feasibility-demonstration of such a measurement.

The Hamiltonian of the δ -kicked accelerator, realized using

a magneto-optic trap (MOT) of laser-cooled atoms that are then released and subjected to pulses from a standing wave of off-resonant light, is

$$\hat{H} = \frac{\hat{p}^2}{2m} + mg\hat{z} - \hbar\phi_d[1 + \cos(G\hat{z})] \sum_{n=-\infty}^{+\infty} \delta(t - nT), \quad (1)$$

where \hat{z} is the position, \hat{p} the momentum, m the particle mass, t the time, T the pulse period, $\hbar\phi_d$ quantifies the strength of the kicking potential, $G = 2\pi/\lambda_{\text{spat}}$, and λ_{spat} is the spatial period of the standing wave applied to the atoms. The quantity g is normally the gravitational acceleration. However, by ‘accelerating’ the standing wave, it is possible to effectively modify g . We have previously used this technique to counteract gravity and regain kicked rotor dynamics [7, 13].

In an innovative analysis by Fishman, Guarneri, and Rebuzzini (FGR) [12], the fact that QAM are observed only when T approaches $\ell T_{1/2} = \ell 2\pi m/\hbar G^2$, where $\ell \in \mathbb{Z}^+$ and $T_{1/2}$ is the half-Talbot time [9], is exploited to yield a dramatically simplified picture of QAM dynamics. In a frame accelerating with g , the linear potential is removed to leave a spatially periodic Hamiltonian. The quasimomentum β is then conserved, i.e., if a momentum state $|p\rangle = |(k + \beta)\hbar G\rangle$, where $k \in \mathbb{Z}$ and $\beta \in [0, 1)$, ‘ladders’ of momentum states of different β evolve *independently*. The resulting n -dependent and β -specific kick-to-kick time evolution operator is

$$\hat{F}_n(\beta) = \exp(-i\{\hat{p} + \text{sgn}(\epsilon)[\pi\ell + \tilde{k}\beta - \gamma(n - 1/2)]\}^2/2\epsilon) \times \exp(i\tilde{k} \cos \hat{\chi}/|\epsilon|), \quad (2)$$

where $\tilde{k} = |\epsilon|\phi_d$, $\tilde{k} = 2\pi T/T_{1/2}$, and $\gamma = gGT^2$. We have introduced a smallness parameter, $\epsilon = 2\pi(T/T_{1/2} - \ell)$, to quantify the closeness of T to $\ell T_{1/2}$ and the dynamical variables are now an angle $\hat{\chi} = G\hat{z}$ and a discrete conjugate momentum $\hat{p} = \hat{p}|\epsilon|/\hbar G$, such that $[\hat{\chi}, \hat{p}] = i|\epsilon|$. If one constructs a kick-to-kick Heisenberg map corresponding to Eq. (2) for the dynamical variables, then in the limit $\epsilon \rightarrow 0$, the commutator vanishes along with the uncertainty principle, and the operators can be replaced by their mean values. Thus

$$\tilde{p}_{n+1} = \tilde{p}_n - \tilde{k} \sin(\chi_n) - \text{sgn}(\epsilon)\gamma, \quad (3a)$$

$$\chi_{n+1} = \chi_n + \text{sgn}(\epsilon)\tilde{p}_{n+1}, \quad (3b)$$

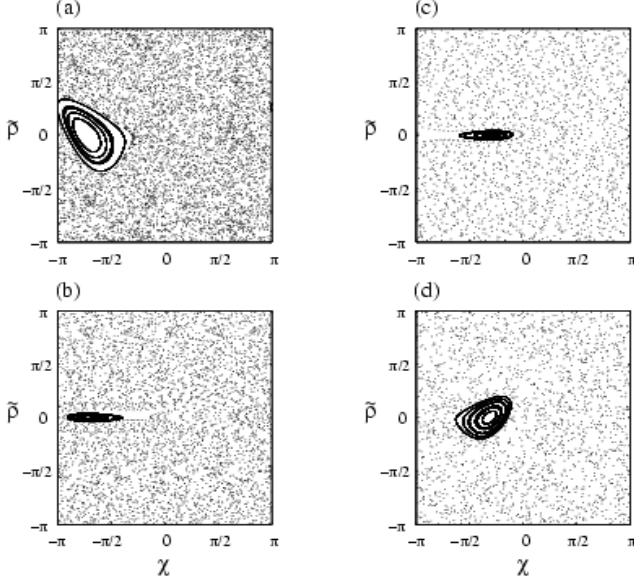


FIG. 1: Phase space plots produced by Eq. (3), when $2\pi\gamma/k^2 = 1/1 \Rightarrow \gamma = (2\pi + \epsilon)^2/2\pi$, and $\tilde{k} = |\epsilon|0.8\pi$ for (a) $\epsilon = -0.88$, (b) $\epsilon = -0.02$, (c) $\epsilon = 0.03$, (d) $\epsilon = 0.6$. This corresponds to $T = 57.4 \mu\text{s}$, $66.5 \mu\text{s}$, $67 \mu\text{s}$, $73 \mu\text{s}$. For (a), (b) the island corresponds to a $(p, j) = (1, 1)$ QAM, and for (c), (d), to a $(p, j) = (1, -1)$ QAM.

where $\theta_n = \langle \hat{\theta}_n \rangle$ and $\tilde{\rho}_n = \langle \hat{\rho}_n \rangle + \text{sgn}[\pi\ell + k\beta - \gamma(n - 1/2)]$. Quantum accelerator modes are one-to-one related to stable periodic orbits of this map [6, 8, 12]. It is very important to note that $\epsilon \rightarrow 0$ coincides with $\hbar \rightarrow 0$ only if $\ell = 0$. Otherwise, as in the experiments here, the classical-particle-like behavior of QAM is due to a quantum resonance effect.

The stable periodic orbits yielded by Eq. (3) (and hence QAM) are classified by their order p and jumping index j (the number of momentum units, in terms of the size of the phase-space cell, traversed after p iterations). The sign of j is determined by whether this is in the positive or negative momentum direction. A necessary condition [12] for the existence of a periodic orbit is $|j/p + \text{sgn}(\epsilon)\gamma/2\pi| \leq \tilde{k}/2\pi$, which can be rewritten (for small ϵ) as

$$-|\epsilon| \left(\frac{\phi_d}{2\pi} + \frac{2\ell\gamma}{k^2} \right) \leq \frac{j}{p} + \text{sgn}(\epsilon)2\pi\ell^2 \frac{\gamma}{k^2} \leq |\epsilon| \left(\frac{\phi_d}{2\pi} - \frac{2\ell\gamma}{k^2} \right). \quad (4)$$

Both ϕ_d and $\gamma/k^2 = gm^2/\hbar^2 G^3$ are independent of T , and therefore of ϵ . Equation (4) is convenient when T is varied from just below to just above $\ell T_{1/2}$, i.e., scanning ϵ from negative to positive, as in the experiments described here. As $\epsilon \rightarrow 0$, the QAM that occur must be characterized by j and p such that $j/p \rightarrow -\text{sgn}(\epsilon)2\pi\ell^2\gamma/k^2$. In general $2\pi\ell^2\gamma/k^2$ is an irrational value, and one usually observes a succession of increasingly high-order QAM as $T \rightarrow \ell T_{1/2}$ [8]. If we tune g so that $2\pi\ell^2\gamma/k^2 = r/s$, where r and s are integers, then $j/p + \text{sgn}(\epsilon)2\pi\ell^2\gamma/k^2 = 0$ for $j/p = -\text{sgn}(\epsilon)r/s$. Once the (p, j) QAM satisfying this condition appears, shifting T closer to $\ell T_{1/2}$ does not result in higher-order QAM.

In a frame accelerating with g , the momentum after N kicks, for an initial condition near a (p, j) stable periodic orbit

[12], in ‘grating recoils’ $\hbar G$ [9] is

$$q_N \simeq q_0 + N \frac{2\pi}{|\epsilon|} \left[\frac{j}{p} + \text{sgn}(\epsilon) \frac{\gamma}{2\pi} \right], \quad (5)$$

where q_0 is the initial momentum. For N a multiple of j , this result is exact for ϵ -classical initial conditions located on (p, j) periodic orbits. We now consider the momentum of orbits specified by $j/p = r/s$ (for $\epsilon < 0$) and $j/p = -r/s$ (for $\epsilon > 0$) as a single function of N and ϵ , in the case where $2\pi\ell^2\gamma/k^2$ approaches rational values. Letting $2\pi\ell^2\gamma/k^2 = r/s + w\ell^2$ [14], we find:

$$q_N \simeq q_0 + N \frac{r}{s} \left(\frac{2}{\ell} + \frac{\epsilon}{2\pi\ell^2} \right) + Nw \left(\frac{2\pi\ell^2}{\epsilon} + 2\ell + \frac{\epsilon}{2\pi} \right). \quad (6)$$

Scanning through ϵ from negative to positive values, one does not generally observe two QAM of the same p and magnitude of j (with positive sign for negative ϵ , and negative sign for positive ϵ) [8, 15]. However, in the gravity-resonant cases we consider, when $2\pi\ell^2\gamma/k^2$ is close to r/s , we always observe an r/s and then a $-r/s$ QAM as we scan ϵ in this way. This is shown in Fig. 1, where we plot Poincaré sections produced by Eq. (3) for $\gamma = k^2/2\pi = (2\pi + \epsilon)^2/2\pi$ (i.e., $r/s = 1$) and $\tilde{k} = |\epsilon|\phi_d = |\epsilon|0.8\pi$ (the approximate experimental mean value [7]). The islands around the $(p, j) = (1, -\text{sgn}(\epsilon)1)$ periodic orbits remain large over a wide range of ϵ and, in dramatic contrast to Ref. [8], no higher-order island structures appear as $\epsilon \rightarrow 0$. In Fig. 2(a) the corresponding QAM are similarly robust and uninterrupted by higher-order QAM as $T \rightarrow T_{1/2}$.

From Eq. (6) we thus see that for a given N , q is a linear function of ϵ whenever $w = 0$. If $w \neq 0$ this changes to a hyperbolic function of ϵ , where the arms of the hyperbolae point in opposite directions for oppositely signed w . Deviation from straight line behavior in a QAM accelerated to a given momentum will be greater for a gravity-resonant mode corresponding to a smaller value of $j/p = r/s$. This is because the acceleration of the mode is $\propto j/p$, but the deviation is $\propto N$. We consider only QAM where $j = r = 1$, so high-order modes exhibit, for a given momentum transfer, greater sensitivity to variations in g than low-order modes.

In our realization of the quantum δ -kicked accelerator, $\sim 10^7$ cesium atoms are trapped and cooled in a MOT to a temperature of $5 \mu\text{K}$, yielding a Gaussian momentum distribution with FWHM $6\hbar G$. The atoms are then released and exposed to a sequence of equally spaced pulses from a standing wave of higher intensity light 15 GHz red-detuned from the $6^2S_{1/2} \rightarrow 6^2P_{1/2}$, ($F = 4 \rightarrow F' = 3$) D1 transition. Hence the spatial period of the standing wave is $\lambda_{\text{spat}} = 447 \text{ nm}$, and $T_{1/2} = 66.7 \mu\text{s}$. The peak intensity in the standing wave is $\simeq 5 \times 10^4 \text{ mW/cm}^2$, and the pulse duration is $t_p = 500 \text{ ns}$. This is sufficiently short that the atoms are in the Raman-Nath regime and hence each pulse is a good approximation to a δ -function kick. The potential depth is quantified by $\phi_d = \Omega^2 t_p / 8\delta_L$, where Ω is the Rabi frequency and δ_L the detuning from the D1 transition. During the pulse sequence, a voltage-controlled crystal phase modulator is used to strobo-

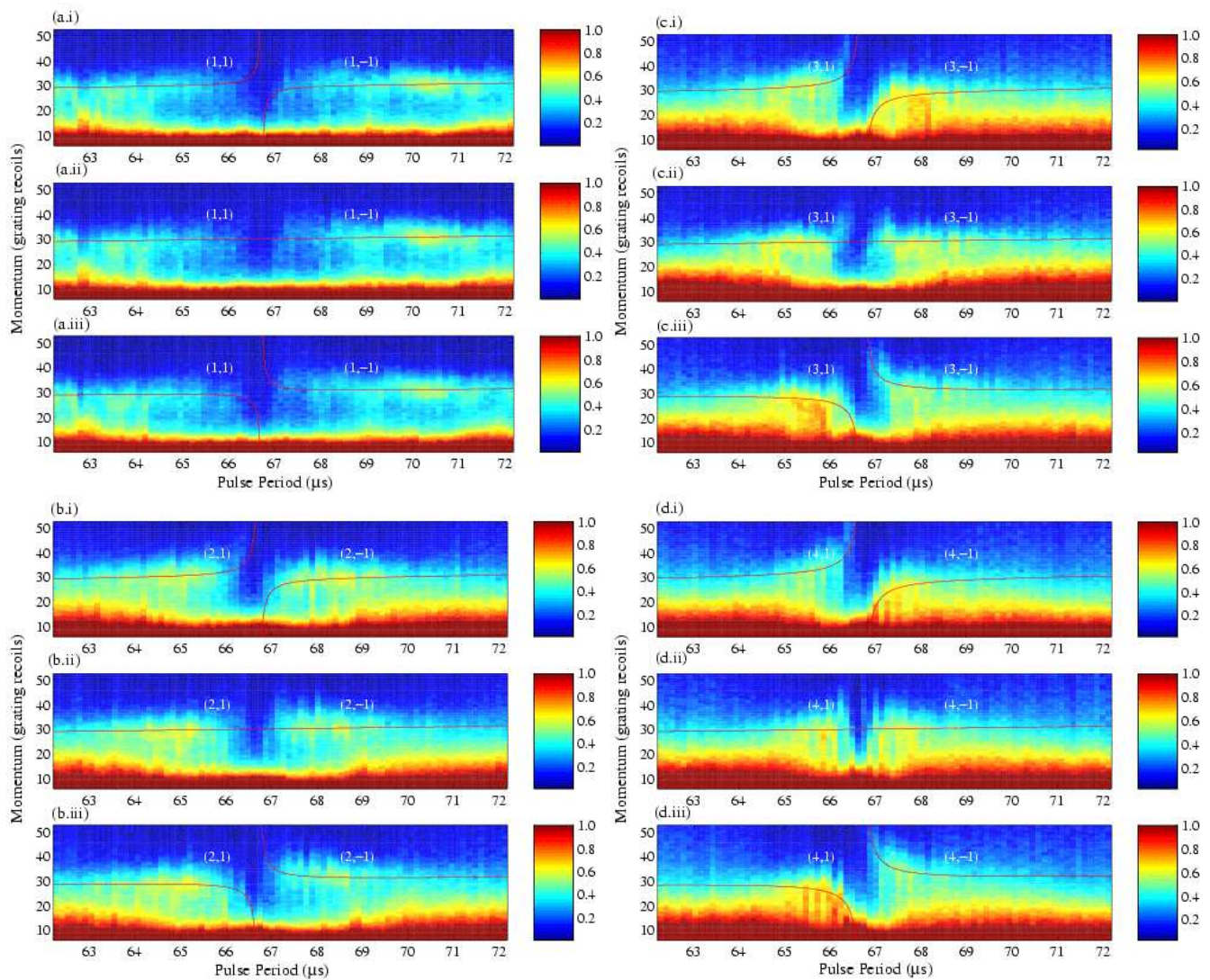


FIG. 2: (color online). Color density plots of experimental momentum distributions for different effective gravity g corresponding to (a) $r/s = 1/1$ (after 15 kicks), (b) $r/s = 1/2$ (30 kicks), (c) $r/s = 1/3$ (45 kicks), and (d) $r/s = 1/4$ (60 kicks), as T is varied in the vicinity of the half Talbot time $T_{1/2} = 66.7 \mu\text{s}$, from $60.5 \mu\text{s}$ to $74.5 \mu\text{s}$ in steps of $0.128 \mu\text{s}$. In each case the QAM corresponds to $j/p = r/s$; subplot (i) corresponds to $w \simeq -8.5 \times 10^{-4}$ (deviation from resonant g is $\sim -8.6 \times 10^{-2} \text{ms}^{-2}$), subplot (ii) to $w \simeq 0$, and subplot (iii) to $w \simeq 8.5 \times 10^{-4}$ (deviation from resonant g is $\sim 8.6 \times 10^{-2} \text{ms}^{-2}$). Overlaid lines, labeled (p, j) , indicate QAM momenta predicted by Eq. (6). Population arbitrarily normalized to maximum value = 1, and momentum defined in a frame falling with g . Note the significantly greater population at high momentum (up to $50\hbar G$) near $T_{1/2}$ in (d.i) and (d.iii), compared to (a.i) and (a.iii).

scopically accelerate the standing wave profile. The atoms therefore effectively experience a non-standard, and controllable, value of gravity. After the pulsing sequence, the atoms fall through a sheet of laser light resonant with the $6^2S_{1/2} \rightarrow 6^2P_{3/2}$, ($F = 4 \rightarrow F'' = 5$) D2 transition, 0.5m below the MOT. By monitoring the absorption, the atoms' momentum distribution is then measured by a time-of-flight method, with resolution $\hbar G$. For further details see Refs. [7, 9].

In Fig. 2 we show momentum distributions for experiments in which the value of T was scanned around $T_{1/2}$ ($\ell = 1$) from $60.5 \mu\text{s}$ to $74.5 \mu\text{s}$, with $2\pi\gamma/k^2$ varied in the vicinity of r/s equal to (a) $1/1$, (b) $1/2$, (c) $1/3$, and (d) $1/4$. To main-

tain the ideal ($w = 0$) total momentum transfer, 15, 30, 45 and 60 kicks were applied, respectively, fixing Nr/s . For each of Figs. 2(a), 2(b), 2(c), and 2(d) the data displayed are: in subplot (ii), from experiments in which $2\pi\gamma/k^2 = r/s$ is fulfilled as exactly as feasible, yielding linear variation of the QAM momentum with T ; and in subplots (i) and (iii), for equal positive and negative deviations, respectively, from this near-ideality, yielding hyperbolic variation of the QAM momentum. Typically $\sim 10\text{--}20\%$ of the atoms are accelerated away from the cloud centered at $p = 0$.

In each subplot (ii) of Fig. 2, the QAM momentum predicted by Eq. (6), shown as an overlaid line, is identical. The

expected linear dependence on T appears to be well confirmed by the data, although the separation of the QAM from the main, non-accelerated cloud, centered at zero momentum, is clearer for smaller $s = p$ (there is less momentum diffusion of the main cloud due to the smaller number of kicks). The effect of imperfectly resonant gravity, shown in subplots (i) and (iii) in Fig. 2, is much more dramatic for larger $s = p$, for which more kicks are applied. In Fig. 2(a), subplots (i) and (iii) are barely distinguishable from subplot (ii), whereas in Fig. 2(d), the momentum distributions in subplots (i) and (iii) are highly asymmetric compared with subplot (ii), with, close to $T_{1/2}$, noticeable population at up to $50\hbar G$. The asymmetry inverts as one changes from below [subplot (i)] to above [subplot (iii)] the resonant value of gravity. We therefore observe a clear qualitative change in the QAM dynamics, highly sensitive to a control parameter. The displayed predictions of Eq. (6) show that deviations from linear behavior only occur when very close to $T_{1/2}$ in Figs. 2(a.i) and 2(a.iii), but are much more significant in Figs. 2(d.i) and 2(d.iii). This is due to the larger number of kicks necessary for large $s = p$ to achieve the same QAM momentum.

The procedure of determining the ‘standing wave acceleration’ at which straight-line behavior of a given (p, j) QAM momentum is observed as a function of T could, in principle, be used as a sensitive atom-optical means of relating h/m [16] to the local gravitational acceleration [17]. This is because $2\pi\ell^2\gamma/k^2 = r/s$ can be rephrased as $g = (h/m)^2(r/s)\lambda_{\text{spat}}^3$ and would be determined by noting when the *total* acceleration (sinusoidal potential plus gravitational) causes these equalities to be fulfilled for a known r/s , and then subtracting the imposed acceleration of the potential. In our setup, where the sinusoidal potential is ‘accelerated’ by using a crystal phase modulator to phase-shift the retroreflected laser beam [7, 9], the value of the phase shift due to a particular applied voltage is difficult to calibrate more precisely than $\sim 1\%$. This accordingly limits our measured precision of the relationship between the local gravitational acceleration and h/m to $\sim 1\%$. Accurate prediction of the QAM momenta for imperfectly resonant values of the effective gravity, as displayed in Fig. 2, is also hampered. This could be improved by a configuration in which a moving sinusoidal potential is formed by two counterpropagating beams with a controllable frequency difference [18], where calibration of the phase shift to between 1ppm and 1ppb is possible. Calibration of λ_{spat} to less than 1ppb is also feasible [17], allowing for the possible sensitive determination of either the local gravitational acceleration [17] or h/m [16], depending on which is known more precisely at the outset. The feasibility of any such scheme will ultimately depend on how precisely the atomic ensemble’s dynamics permit the determination of the acceleration of the sinusoidal potential for which the resonant, linear with T , behavior of the QAM occurs. Ascertaining this will require substantial theoretical and experimental investigation.

In conclusion, we have observed qualitative changes in the

motional quantum dynamics of cold cesium atoms, which are highly sensitive to the precise value of an externally adjustable parameter, the effective gravity. This is distinct from conceptually related proposals that consider slightly differing Hamiltonians to study the Loschmidt echo or fidelity, and demonstrates an attractive link to the concepts of highly sensitive dynamics in classically chaotic systems. Furthermore, we have described a feasible experimental scheme taking advantage of this sensitivity to determine a relationship between the local gravitational acceleration and h/m .

We thank K. Burnett, S. Fishman, I. Guarneri, L. Rebuzzini, G.S. Summy, and particularly R.M. Godun, for very helpful discussions. We acknowledge support from the Clarendon Bursary, the UK EPSRC, the Royal Society, the EU through the TMR ‘Cold Quantum Gases’ Network, the Lindemann Trust, and NASA.

-
- [1] F. Haake, *Quantum Signatures of Chaos* (Springer, Berlin, 2001), 2nd ed.
 - [2] F.M. Cucchietti *et al.*, Phys. Rev. E **65**, 046209 (2002); R.A. Jalabert and H.M. Pastawski, Phys. Rev. Lett. **86**, 2490 (2001).
 - [3] N.R. Cerruti and S. Tomsovic, Phys. Rev. Lett. **88**, 054103 (2002); Y.S. Weinstein, S. Lloyd, and C. Tsallis, *ibid.* **89**, 214101 (2002); G. Benenti and G. Casati, Phys. Rev. E **65** 066205 (2002).
 - [4] A. Peres, *Quantum Theory: Concepts and Methods* (Kluwer Academic Publishers, Dordrecht, 1993); R. Schack and C.M. Caves, Phys. Rev. E **53**, 3257 and 3387 (1996); G. Garcia de Polavieja, Phys. Rev. A **57**, 3184 (1998).
 - [5] S.A. Gardiner, J.I. Cirac, and P. Zoller, Phys. Rev. Lett. **79**, 4790 (1997).
 - [6] S. Schlunk *et al.*, Phys. Rev. Lett. **90**, 054101 (2003).
 - [7] M.B. d’Arcy *et al.*, Phys. Rev. E **64**, 056233 (2001).
 - [8] S. Schlunk *et al.*, Phys. Rev. Lett. **90**, 124102 (2003).
 - [9] R.M. Godun *et al.*, Phys. Rev. A **62**, 013411 (2000).
 - [10] M.K. Oberthaler *et al.*, Phys. Rev. Lett. **83**, 4447 (1999); M.B. d’Arcy *et al.*, Phys. Rev. A **67**, 023605 (2003).
 - [11] S. Fishman in *Quantum Chaos*, Proceedings of the International School of Physics ‘Enrico Fermi’, course CXIX, edited by G. Casati, I. Guarneri, and U. Smilansky (IOS Press, Amsterdam, 1993); R. Graham, M. Schlautmann, and P. Zoller, Phys. Rev. A **45**, R19 (1992); F.L. Moore *et al.*, Phys. Rev. Lett. **75**, 4598 (1995).
 - [12] S. Fishman, I. Guarneri, and L. Rebuzzini, Phys. Rev. Lett. **89**, 084101 (2002); J. Stat. Phys. **110**, 911 (2003).
 - [13] M.B. d’Arcy *et al.*, Phys. Rev. Lett. **87**, 074102 (2001); Phys. Rev. E **69**, 027201 (2004).
 - [14] We have multiplied out a singularity occurring for q at $\epsilon = 0$ when $w = 0$.
 - [15] The sign of j used here is consistent with that used for the gravitational potential, and the definition of j in Ref. [12].
 - [16] S. Gupta *et al.*, Phys. Rev. Lett. **89**, 140401 (2002).
 - [17] A. Peters, K.Y. Chung, and S. Chu, Nature (London) **400**, 849 (1999).
 - [18] J. Hecker Denschlag *et al.*, J. Phys. B **35**, 3095 (2002)